PEER INGEO 2017 REVIEWED

Synchronization routine for real-time synchronization of robotic total stations

Zan GOJCIC†, Slaven KALENJUK[1], Werner LIENHART[1]

†ETH Zürich, Institute of Geodesy and Photogrammetry
Zurich, Switzerland
E-mail: zan.gojcic@geod.baug.ethz.ch

[1] Graz University of Technology, Institute of Engineering Geodesy and Measurement Systems
Graz, Austria
E-mail: slaven.kalenjuk@tugraz.at, werner.lienhart@tugraz.at

Abstract

Large geodetic projects often require measurement configurations with multiple robotic total stations (RTSs). In order to combine the observables of the spatially separated RTSs, a common time frame has to be established. In this paper, we introduce a novel synchronization routine for relative, real-time synchronization of multiple RTSs. The proposed routine, consisting of two main steps, is independent of ambient conditions and requires no additional hardware.

In the first part, we analyze the characteristics of the RTS's internal time at stable meteorological conditions by comparing it to the reference time established using a dedicated GNSS receiver. Referring to the findings, we propose a calibration procedure for the temperature calibration of the RTS's internal time. We determine the drift rate at different temperatures in dedicated experiments within a climate chamber and derive a calibration function from this data.

In the second part, we apply the calibration function in practical measurements and show its applicability for selected RTSs at variable temperatures. As demonstrated in two experiments, the proposed drift compensation combined with a cross-correlation based initial time delay estimation (TDE), proves to be a reliable approach for the time synchronization of spatially separated RTSs. After the measurement duration of eight hours, the RTSs are synchronized within one sampling interval, i.e. better than 50 ms.

Key words: Real-time synchronization, robotic total stations, cross-correlation, temperature calibration

1 INTRODUCTION

Since several years, kinematic measurements using RTSs are commonly used in many fields of engineering geodesy. Modern RTSs are multi-sensor systems, which combine angle and distance measurements with compensator and automatic fine aiming data for output of three-dimensional coordinates. In static mode, the synchronization of the individual subsystems is not critical, but in kinematic mode, the insufficient synchronization leads to systematic errors in the calculated coordinates (Stempfhuber, W. 2004). Early work in the time synchronization field aimed at the internal synchronization of these subsystems and as a result, RTSs nowadays enable internal synchronization of individual subsystems within 1 ms of each other (Stempfhuber, W. and Wunderlich, T. 2004; Stempfhuber, W. 2009). However, demanding geodetic projects usually require system configurations, consisting of multiple, spatially separated RTSs. In order to synchronize the output of individual instruments in a sensor network, a common time frame has to be established.

We adopt the notation from Hennes et al. (2014), where synchronization methods are divided into trigger-based, event-based and numerical methods. In trigger-based methods, external software or hardware triggers are used to trigger measurements of all sensors simultaneously. If the sensors do not enable direct hardware triggering (e.g. PPS events of dedicated GPS timing receivers), as it is the case with today's RTSs, the synchronization accuracy is influenced by the accuracy of the transfer and dead time estimation. Moreover, in order for the GPS receiver to synchronize with the GPS time, a clear view of the sky has to be ensured, which limits the applicability of the method to outdoor cases.

In event-based methods (e.g. Cristian, F. 1989) synchronization is achieved by timestamping each event at the slave (i.e. sensors) and at the master (i.e. computer used for the remote control) and respectively deriving their time offset. In a spatially separated network, computers, which exhibit different drift rates, are used for remote control of the sensors. They can be synchronized, for instance, using the network time protocol (NTP), but this limits the applicability of the method to cases where the computers are connected to the internet, or it requires setting up a stratum 0 time server locally (Mills, D. L. 2006).

In numerical methods, each measurement is saved with the corresponding time stamp. This information is used for the TDE, e.g. with the generalized correlation method proposed by Knapp and Carter (1976). By estimating the time delay, the sensors are synchronized at that point in time but may drift apart with time due to different drift rates. Additionally, the highest obtainable resolution of the TDE is limited to the sampling interval of the measurements.

In this paper, we introduce a time synchronization routine for synchronization of modern RTSs, which combines the cross-correlation based TDE with a calibration function used to compensate the time drift of the internal time. In experiments, we demonstrate the practical applicability of our synchronization routine for real-time synchronization of two spatially separated RTSs. The routine enables the synchronization of the instruments within one sampling interval (i.e. approx. 50 ms) after eight hours of measurement duration, requires no additional software and is independent of ambient conditions.

2 INVESTIGATION OF THE TOTAL STATION'S INTERNAL TIME

To obtain the aspired synchronization accuracy, the synchronization routine has to consider the characteristics of the instrument's internal time. Therefore, we investigated the internal time behavior of several total stations (TSs). We describe our method for determining the drift

rate of the TS's internal time and discuss drift rates of selected Leica Geosystems TSs in Section 2.1. Based on the results, we select two motorized instruments, which have the highest drift rate difference and determine their internal, temperature dependent, time calibration function (Section 2.2).

2.1 INTERNAL TIME CHARACTERISTICS AND DRIFT ESTIMATION

During the internal time drift estimation, selected TSs were remote controlled using the GeoCOM communication interface. We selected GeoCOM command *TMC_GetAngle1*, as it is independent of the internal synchronization and returns the time stamp of the angle measurement with millisecond resolution. In Leica TSs, angle measurements are not carried out query-based, but are updated internally with an update frequency of approximately 20 Hz (Lienhart, et al. 2017). This routine results in an arbitrary dead time of the measurements $\Delta t_{qry.}^{res.}$ (see Figure 1), which denotes the time between the query and the following measurement and has a value between zero and the sampling interval of the measurement.

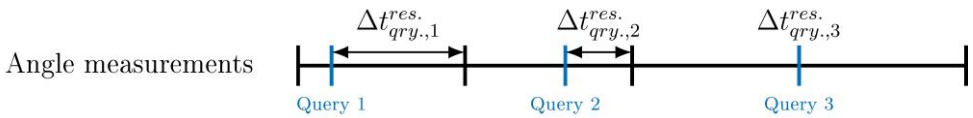

Figure 1: Dead time of the angle measurement

The dead time of the measurement naturally reflects itself in the measurement duration, which we define as the time difference between the CPU time stamp of the transmitted GeoCOM command and the CPU time stamp of the received GeoCOM response (Figure 2)

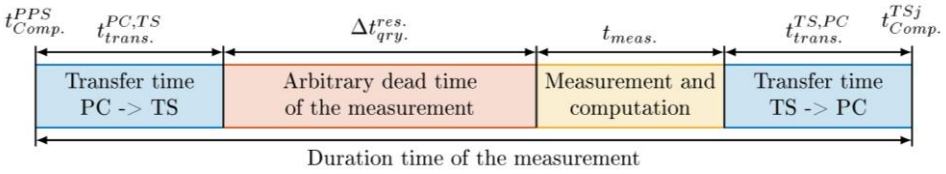

Figure 2: Duration time of the measurement

In order to determine the internal time drift rate, all individual parts of the measurement duration have to be estimated. Knowing the length of the GeoCOM command and response strings, both transfer times can be calculated as

$$t_{trans.} = \frac{m_{char.} n_{bits}^{char.}}{baudrate}, \tag{1}$$

where $m_{char.}$ denotes the number of characters in the string and $n_{bits}^{char.}$ the number of bits per individual character. Since the measurement and its computation are carried out internally and no significant CPU load changes are expected, we consider them constant. Thus, the arbitrary dead time of the measurements remains the only parameter to be estimated from the registered measurement duration. Based on the characteristics of the internal time, we estimate the drift rate of the RTS by periodically computing its time offset to the GPS time, provided in form of a PPS event by the dedicated GPS timing receiver, over a longer period of time. The time offset of the RTS j to the GPS time at epoch i $\Delta t_{GPS}^{TSj}(i)$ is

$$\Delta t_{GPS}^{TSj}(i) = \left[t_{TSj}^{Meas.}(i) - t_{GPS}^{PPS}(i) \right] - \left[t_{Comp.}^{TSj}(i) - t_{Comp.}^{PPS}(i) \right] + t_{trans.}^{TS,PC}(i), \tag{2}$$

where $t_{TSj}^{Meas.}$ denotes the time stamp of the measurement in TS's internal time, t_{GPS}^{PPS} denotes the GPS time stamp of the PPS event, $t_{Comp.}^{TSj}$ and $t_{Comp.}^{PPS}$ denote CPU time stamp of the GeoCOM response and CPU time stamp of the PPS event respectively and $t_{trans.}^{TS,PC}$ denotes the transfer time from the TS to the PC. Under the assumption of a linear dependency of the time offset on the duration time at a constant temperature, a linear regression analysis can be performed. Following this procedure, we carried out drift rate experiments with seven Leica TSs at stable meteorological conditions with constant ambient temperature of about 25°C. The results are summarized in Table 1. In comparison to drift rates of TS11 and TS15 instruments (typically between 0 and -7 ppm), TS16 and MS60 instruments show higher drift rates (between -36 and -58 ppm). A time drift of -58 ppm corresponds to a time error of 1.7 seconds at the end of the 8 h experiment duration. For the in-depth analysis we selected one instrument from each group, namely a Leica TS15 and a Leica MS60.

Table 1: Results of the drift rate experiment for selected TSs

Instrument	SN	Duration [h]	b [ppm]	σ_r [ms]
Leica TS11	1661948	3	-5.4	2.5
Leica TS11	1663286	6	-0.4	3.5
Leica TS11	1663297	4	-0.9	3.4
Leica TS15	1613987	8	-7.1	1.4
Leica TS16	3010090	6	-36.3	5.4
Leica TS16	3011220	6	-45.3	5.3
Leica MS60	882001	8	-57.9	1.3

2.2 CALIBRATION ROUTINE AND TEMPERATURE DEPENDENT TIME CALIBRATION FUNCTION

Crystal oscillators are electrical circuits, used for generation of the sinusoidal waveform, where a piezo-electric crystal, usually a quartz crystal, controls the frequency of the waveform (Amos, S. W. and Amos, R. S. 2002). They are commonly used to keep track of time in electronic devices. To keep an accurate track of time, the frequency of the oscillator has to be as stable as possible. Most electronic devices use an AT-cut quartz crystal, which shows a cubic dependence of frequency on temperature (Frerking, M. E. 1978, p. 130). At short time intervals, the stability of the oscillator's frequency is mostly affected by temperature changes. This is also true for the selected total stations as was confirmed by dedicated temperature investigations. Referring to the findings, we propose a temperature calibration procedure for the temperature calibration of the RTS's internal time. The proposed calibration procedure consists of three steps.

Drift rate experiments performed in a climate chamber: Drift rate experiments are carried out at constant temperatures in equally distributed temperature steps[1] from 0°C to 50°C. Constant temperature at each temperature steps can be ensured by using a climate chamber. We select temperature steps of 10°C and a duration time of 6 hours for individual experiments[2]. During these tests the internal temperature of the instrument is permanently queried using the GeoCOM command *CSV_GetIntTemp*.

Estimation of the calibration function: A cubic model, dependent on the internal temperature is fitted to the linear regression coefficients (drift rates at individual temperature steps) using least squares adjustment. The obtained calibration function can be used to

[1] Due to the limitations of the used climate chamber (Memmert ICP400), tests at below 0°C were not performed.
[2] Note, that smaller temperature steps would increase the accuracy of the calibration function.

calculate the temperature correction term k for the individual time stamp of the RTS's internal time as

$$k(i) = a_3 T_{Internal}(i)^3 + a_2 T_{Internal}(i)^2 + a_1 T_{Internal}(i) + a_0. \quad (3)$$

Evaluation of the calibration function: Applicability of the calibration function is evaluated by comparing calibrated time stamps of the internal time to a reference time, during an experiment at variable temperature.

This proposed calibration procedure was carried out for selected RTSs (see Section 2.1). The obtained calibration functions are depicted in Figure 3 and the coefficients of the 3rd order polynomial are listed in Table 2. Aside from the offset, the internal time source of the selected RTS exhibit similar (cubic) temperature dependence.

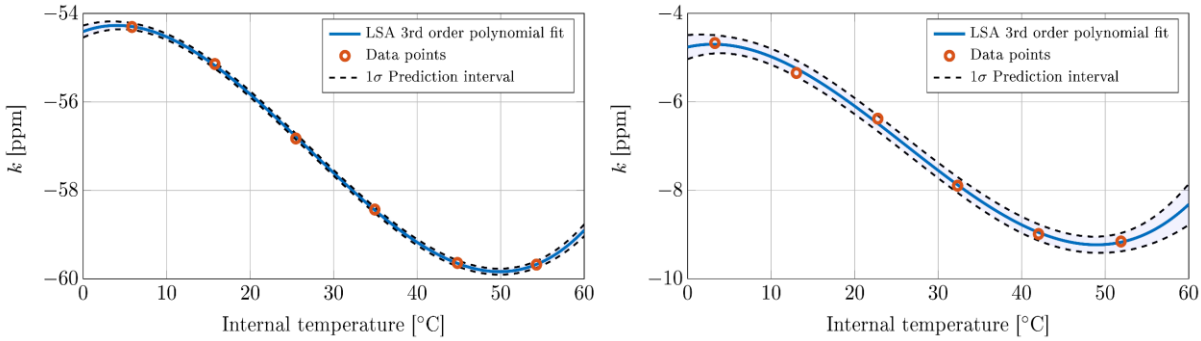

Figure 3: Calibration function of Leica MS60 (left) and Leica TS15 (right)

Table 2: Coefficients of the calibration function

Instrument	SN	a_0	$a_1[°C^{-1}]$	$a_2[°C^{-2}]$	$a_3[°C^{-3}]$
Leica MS60	882001	-4.7623	0.0419	-0.0073	0.00009
Leica TS15	1613987	-54.4086	0.0698	-0.0093	0.00010

The applicability of the calibration functions was evaluated with an experiment at controlled environment. Variations of the temperature were simulated using a climate chamber and a dedicated timing GPS receiver was used for reference time measurements. Using the obtained calibration function, the internal time drift rate of the Leica MS60 is reduced from 58.15 ppm (more than 2.5 seconds after 12 h) to 0.29 ppm (less than 0.013 seconds after 12 h). Improvements can also be achieved for the Leica TS15 where the drift rate can be reduced from 7.54 ppm to 0.29 ppm (Figure 4, Table 3).

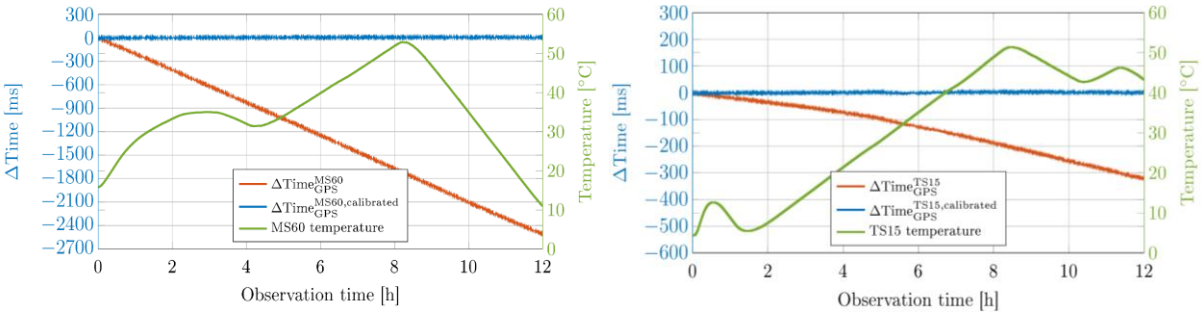

Figure 4: Evaluation of the Leica MS60 (left) and Leica TS15 (right) calibration function at variable temperature

Table 3: Results of the calibration function evaluation at variable temperatures

Instrument	Time source	Duration [h]	$\max(\lvert\Delta t^{GPS}_{Instrument}\rvert)$ [ms]
Leica MS60	Raw internal	12	2512.06
	Calibrated	12	12.43
Leica TS15	Raw internal	12	325.77
	Calibrated	12	12.33

3 SYNCHRONIZATION ROUTINE

Based on the findings from the RTS internal time investigation (see Section 2) we propose a synchronization routine for real time synchronization of RTSs. The proposed routine combines the initial TDE with the calibration function for compensation of the time drift. We evaluate the performance of the proposed routine during two experiments at variable temperature.

3.1 TWO STEP SYNCHRONIZATION ROUTINE

The proposed synchronization routine is divided into two parts (Figure 5). In the first part, the initial time offset of RTSs is determined as the time offset τ that maximizes the cross-correlation function (CCF) of the vertical angle measurement time series[3]. A TDE is performed using time stamps of the internal time. Therefore, the estimation of the transfer time delay and the dead time can be omitted. To improve the correlation properties of the measurements, an artificial signal (approximation of the Dirac impulse) is generated by manually moving a dedicated prism[4] up and down. Note that the highest obtainable resolution of the cross-correlation based TDE equals the sampling interval of the measurements. Therefore, in the first part of the routine, the measurement mode with the highest sampling rate is selected. Namely, angle-only measurements performed using GeoCOM command *TMC_GetAngle1* with Leica TS15 and full measurements performed using GeoCOM command *TMC_GetFullMeas* with Leica MS60 (Lienhart, W. et al. 2017). Additionally, CCF is subsample interpolated using the parabola-based method (Jacovitti, G. and Scarano, G. 1993). If the synchronization is performed in post-processing, the first part of the synchronization routine can be repeated at the end of the measurement and a linear trend of the synchronization error can be derived and used to further improve the synchronization accuracy.

In the second part of the routine, RTSs switch back to the predefined measurement mode. Immediately after each measurement, the internal temperature of the instrument is queried. The internal temperature provides the best estimation of the crystal oscillator's temperature and requires no additional hardware. Internal temperature reading is used to calculate the time correction parameter using Equation 3 and thus the calibrated time stamp follows as

$$t_{Calibrated}(i) = t_{Calibrated}(i-1) + \left[t_{Internal}(i) - t_{Internal}(i-1)\right]\left[1-k(i)\right] \quad (4)$$

The second part of the synchronization routine is repeated until the end of the measurement campaign. Based on the aspired accuracy, it is recommended to repeat the first part of the routine at regular intervals in case of very long measurement campaigns. By repeating the first part of the routine, the time offset is determined anew and the synchronization error is set back to zero.

[3] Based on the measurements configuration, horizontal angle measurement could also be used for determination of the initial time offset.
[4] During the first step, RTS have to be locked on the same, dedicated prism.

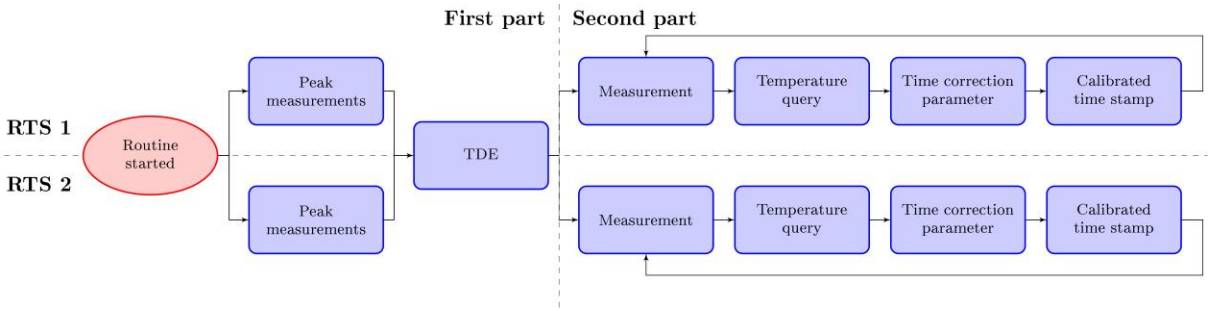

Figure 5: Synchronization routine architecture

3.2 EVALUATION OF THE SYNCHRONIZATION ROUTINE

The performance of the proposed synchronization routine was evaluated in the course of two experiments on the measurement roof of the TU Graz geodesy building (see Figure 6). To investigate the long-term applicability of the temperature dependent calibration functions, the second experiment was performed three months after the first experiment. In the time between the experiments, various other measurements were performed with the selected RTSs to simulate the real use case. The duration of the experiments was selected based on the normal duration of a one-day project, i.e. eight hours. At the start of each experiment, the RTSs were synchronized using the proposed synchronization routine. Theoretically, error free synchronization would lead to zero time offset between the RTSs at the end of the experiment. Therefore, the performance of the synchronization can be assessed directly, by performing the cross-correlation based TDE at the end of the experiment (see Figure 7).

For the generation of the artificial peak in the vertical angle measurements a single dedicated prism was used (see Figure 6). In such a measurement configuration, the possibility of direct reflections of the ATR or EDM signal from the front surface of the prism has to be taken into consideration, especially at small angles of incidence. According to Lackner and Lienhart (2016) measurements to the used circular prism Leica GPR121 are not affected by the reflection from the front surface, due to the anti-reflex coating of the prism. We observed a maximum temperature change of $2.5°C$ during the first and $9.5°C$ during the second experiment.

Quantitative results of both experiments are shown in Table 4. Using the proposed synchronization routine, we can reduce the synchronization error from 1093.3 ms in the first experiment and 1393.0 ms in the second experiment to 36.0 ms and -30.7 ms respectively. The impact of the improvements can be observed by comparing the time series of the vertical measurements at the end of the experiment (see Figure 8).

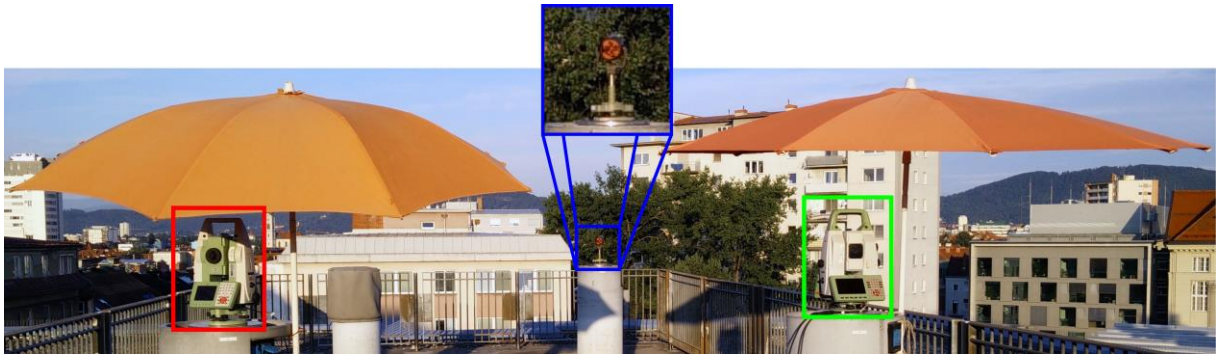

Figure 6: Measurement configuration of the evaluation experiments (red - Leica TS15, green - Leica MS60, blue - dedicated prism)

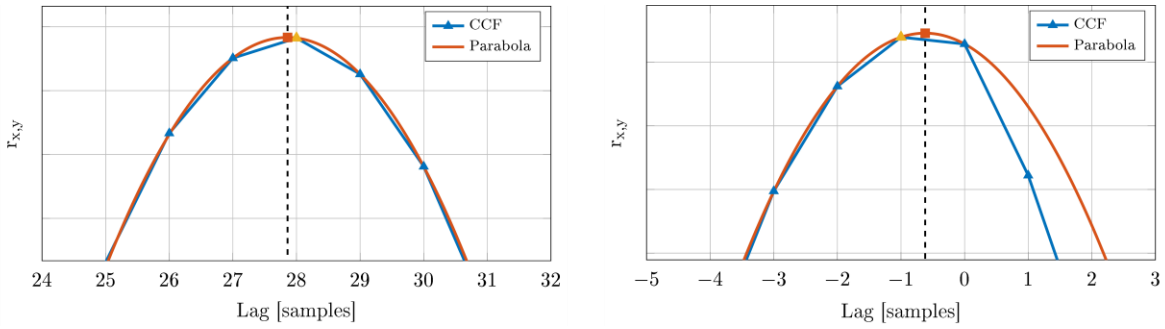

Figure 7: CCF with the parabola-based subsample interpolation (one sample equals 50 ms). Orange triangle depicts the maximum of CCF and red square the maximum of the parabola (raw internal time left, calibrated internal time right).

Table 4: Results of the evaluation experiments

	Source	Duration [h]	Δt_{RTS1}^{RTS2} [ms]
1. experiment	Raw internal time	8	1093.3
	Calibrated time	8	36.0
2. experiment	Raw internal time	8	1393.0
	Calibrated time	8	-30.7

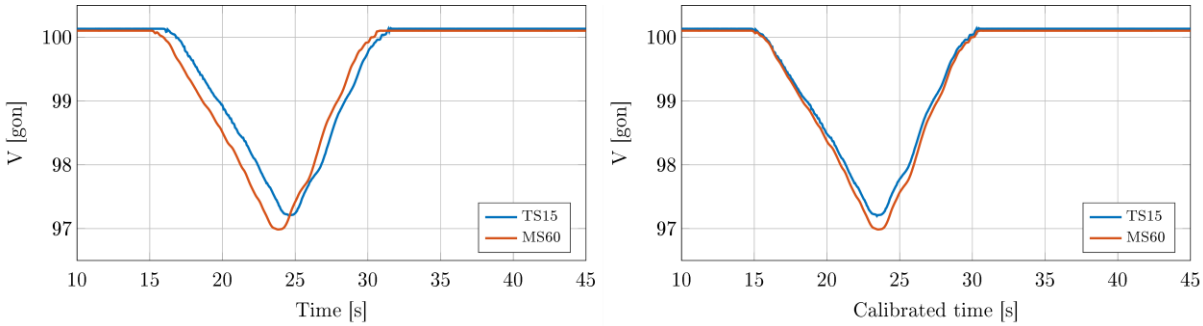

Figure 8: Vertical angle measurement at the end of the second experiment (raw internal time left, calibrated internal time right)

4 CONCLUSION

In this work, we propose a new calibration procedure for temperature calibration of the internal time of robotic total stations. The proposed synchronization routine is based on an initial time offset estimation using CCF in combination with the drift correction using the internal temperature of the instrument together with a calibration function derived from laboratory experiments. The obtained calibration function is later used as part of the proposed synchronization routine for real time synchronization of two RTSs. Our routine requires no additional hardware and also works in changing ambient conditions. We demonstrate that after eight hours of measurement time, two RTSs can be synchronized within one sampling interval, i.e. better than 50 ms.

The proposed routine was developed using Leica instruments, but the basic idea can be adapted to any modern RTS, which enables remote control, returns time stamps of the measurements and allows internal temperature queries.

REFERENCES

Amos, S. W. – Amos, R. S. 2002. Newnes Dictionary of Electronics, Fourth edition. Newnes, Oxford, England. 389pp.

Cristian, F. 1989. Probabilistic clock synchronization. In *Distributed Computing*, Vol. 3. 1989, pp. 146-158.

Frerking, M. E. 1978. Crystal Oscillator Design and Temperature Compensation. Van Nostrand Reinhold, New York, NY, USA. 240 pp.

Hennes, M. – Urban, S. - Wursthorn, S. 2014. Zur Synchronisierung von Multi-Sensor-Systemen – Grundlagen und Realisierung. In *DVW-Schriftreihe*, Vol. 75. 2014, pp. 25-37.

Jacovitti G. – Scarano G. 1993. Discrete Time Techniques for Time Delay Estimation. In *IEEE Transaction on Signal Processing*. Vol. 41, No. 2. pp 525-533.

Knapp, C. H. – Carter, G. C. 1976. The Generalized Correlation Method for Estimation of Time Delay. In *IEEE Transaction on Acoustics, Speech and Signal Processing.* Vol.

ASSP-24, No. 4. pp. 320-327.

Lackner S. – Lienhart W. 2016. Impact of Prism Type and Prism Orientation on the Accuracy of Automated Total Station Measurements. Proc. *Joint International Symposium on Deformation Monitoring (JISDM)*. 8p.

Lienhart. W. – Ehrhart M. – Grick M. 2017. High Frequent Total Station Measurements for the Monitoring of Bridge Vibrations. In *Journal of Applied Geodesy*. Vol. 11. 2017 pp. 1-8.

Mills, D. L. 2006. Computer Network Time Synchronization - the Network Time Protocol. CRC Press. 304pp.

Stempfhuber, W. 2004. Ein integritätswahrendes Messsystem für kinematische Anwendungen. PhD thesis, Institut für Geodäsie, GIS und Landmanagement, TU Munich,Germany. 131pp.

Stempfhuber, W. – Wunderlich, T. 2004. Auf dem Weg zur Sensorsynchronisation von GPS und TPS für kinematische Messaufgaben. In *Allgemeine Vermessungs-Nachrichten.* Vol. 5. pp. 175-184.

Stempfhuber, W. 2009. Verification of the Trimble Universal Total Station (UTS) Performance for Kinematic Applications. In *Grün/Kahmen (Eds), Optical 3-D Measurement*

Techniques IX, Vienna, FIG Commission 5 and 6, IAG Special Commission 4, ISPRS

Commission 5. pp. 211-221.